

11-02  
393 240

# TECHNICAL NOTE

D-1074

RADIATIVE HEAT TRANSFER DURING ATMOSPHERE

ENTRY AT PARABOLIC VELOCITY

By Kenneth K. Yoshikawa and Bradford H. Wick

Ames Research Center  
Moffett Field, Calif.

NATIONAL AERONAUTICS AND SPACE ADMINISTRATION

WASHINGTON

November 1961



## NATIONAL AERONAUTICS AND SPACE ADMINISTRATION

---

TECHNICAL NOTE D-1074

---

## RADIATIVE HEAT TRANSFER DURING ATMOSPHERE

ENTRY AT PARABOLIC VELOCITY<sup>1</sup>

By Kenneth K. Yoshikawa and Bradford H. Wick

## SUMMARY

Stagnation point radiative heating rates for manned vehicles entering the earth's atmosphere at parabolic velocity are presented and compared with corresponding laminar convective heating rates. The calculations were made for both nonlifting and lifting entry trajectories for vehicles of varying nose radius, weight-to-area ratio, and drag. It is concluded from the results presented that radiative heating will be important for the entry conditions considered.

## INTRODUCTION

The purpose of this paper is to provide an assessment of the importance of radiative heating in the design of manned vehicles entering the earth's atmosphere at parabolic velocity.

In making the assessment of the importance of the radiative heat transfer, the available data on the emissivity of high temperature air was applied to calculate the stagnation-point radiative heating for a number of parabolic entry vehicles and entry conditions. Corresponding values of convective heating were also determined.

## METHOD

The geometry and flow equation used for calculating the stagnation-point radiative heating rates are shown in figure 1. The shaded portion of the gas cap radiates to the stagnation point. The transfer of heat is, in detail, a complicated process. For our purposes, however, certain assumptions could be made which lead to the simple equation shown for the radiative heating rate at the stagnation point. The factor  $\delta$  in the equation is the shock standoff distance, and the factor  $E_t$  is the total energy being radiated per unit time from each unit volume. The factor of  $1/2$  is to account for the fact that only one-half the total energy leaves each side of a thin shock layer.

---

<sup>1</sup>The information in this report was a part of the material in the paper entitled "Radiative Heat Transfer at Parabolic Entry Velocity" by Yoshikawa, Wick and Howe, which was presented at the Joint Conference on Lifting Manned Hypervelocity and Reentry Vehicles, Langley Field, Virginia, April 11-14, 1961. (Mr. Howe's contribution to the original conference paper which concerned the use of gas injection to reduce radiative heat transfer is not included in the present report since a comprehensive treatment of this general problem has now been presented by Mr. Howe in NASA Technical Report R-95).

Appendix A summarizes (1) the assumptions upon which the equation is based, (2) the procedures and information used in applying the equation, and (3) the limitations and probable accuracy of the estimates. Also given in appendix A are the stagnation-point radiative heating rates for a wide range of velocities and altitudes and a comparison of the rates with the corresponding stagnation-point laminar convective heating rates. Appendix B defines the symbols used in this paper. As indicated in appendix A, the accuracy of the radiative heating estimates is limited by uncertainties as to the accuracy and applicability of the values of  $E_t$  used. The particular values of  $E_t$  used are for air in equilibrium behind the shock wave. As noted in appendix A, the use of equilibrium values of  $E_t$  appears to be satisfactory for a number of parabolic velocity entry vehicles and entry conditions. A factor of uncertainty of 2 appears to be a possibility for the equilibrium values of  $E_t$ . There is a distinct possibility, however, of nonequilibrium radiation for some vehicles, depending upon their geometry and weight. In this event, the radiation rates could be at least an order of magnitude higher than those for equilibrium conditions. Granting that there are these uncertainties connected with the radiative heating estimates, it is believed, however, that they are useful in two respects. The estimates can be used to provide a qualitative answer as to the importance of radiative heat transfer for parabolic velocity entries and, also, provide a good indication of the vehicle parameters which influence the radiative heat transfer.

The radiative and convective heating rate estimates for parabolic entry velocity were for the single-pass undershoot type of entry limited to a maximum deceleration of 10 g. (For a further description of the undershoot type of entry, see ref. 1.)

## RESULTS AND DISCUSSION

Some of the estimates for zero-lift entries are given in figure 2. The maximum radiative heating rate is plotted in Btu/sec-sq ft as a function of nose radius in feet. The dashed curve is for spheres of varying radius, and the solid curve is for a blunt body consisting of a cylinder with nose shapes of varying radius. The nose shapes were derived by progressively blunting a  $45^\circ$  half-angle cone until finally the nose was only a spherical segment. Both heating rate curves are for zero lift-drag ratio, parabolic entry velocity, and a vehicle loading of 100 lb/sq ft. Also shown in the figure is a simple equation for the maximum radiative heating rate. The equation was empirically derived from our heating rate estimates for a number of zero-lift entries. (Limitations to the use of this equation are given in appendix A.) The equation shows that the radiative rate varies directly with the vehicle nose radius and roughly as the square of  $W/A$  and  $1/CD$ . The maximum radiative heating rate curve for the spheres illustrates the linear relationship between heating rate

and  $R$  that exists when the other two factors are constant. The blunt-body curve illustrates the effect of a coupling between nose radius and  $C_D$  for the case of a practical vehicle of a given weight and area. In this case an increase in nose radius causes an increase in  $C_D$ . Consequently, the apparent effect of nose radius is much less than that for the spheres. Maximum convective heating rates for the two cases are shown in figure 3. These are for equilibrium laminar boundary-layer conditions. Also shown in the figure is the simple equation for maximum convective heating rate. A comparison of the equations for the two types of heating shows that they are functions of the same vehicle factors. However, the factors have a more powerful influence in the case of radiative heating.

It is also of interest to compare the maximum radiative and convective rates for the blunt-body case. To make this comparison easier, the blunt-body curves have been transposed to figure 4. The radiative rate ranges from a small fraction of the convective for a 2-foot radius to nearly equal to the convective for a 10-foot radius. The change with nose radius is due more to the reduction in convective heating than to the increase in radiative heating.

Next to be considered are the time histories of the heating rates and the heat absorbed at the stagnation point during the complete entry. The pertinent features of the time histories can be briefly stated. The radiative and convective rates peaked at nearly the same time and the period of the radiative heating was about  $1/3$  of that for the convective. The radiative and convective heat absorbed at the stagnation point during the complete heating periods are shown in figure 5. Here the heat absorbed in Btu/sq ft is plotted as a function of nose radius for the blunt-body case. The trends of these curves are found to be similar to the heating rate curves. The ratio of radiative heat to convective heat for a given nose radius is less than the corresponding ratio for the heating rates because the period of the radiative heating was shorter than that for the convective heating.

Another factor of importance in assessing the radiative heating contribution is the total heat absorbed during entry. In order to provide values of total heat absorbed it was necessary to make some approximations in the case of radiative heating. It was found that for the 2-foot-radius nose, the total radiative heat absorbed was less than 5 percent of the convective, and in the case of the 10-foot-radius nose the total radiative heat was about 25 percent of the convective. This increase in percentage in going from the 2-foot to the 10-foot radius was almost entirely due to a change in total radiative heat absorbed.

In considering the effect of  $L/D$  on stagnation-point radiative heating rates, one should account for the interrelationship of  $L/D$  and the pertinent vehicle parameters; namely, nose radius  $R$ , weight-to-area ratio  $W/A$ , and drag coefficient  $C_D$ . It is not possible to select completely typical variations of the vehicle parameters with  $L/D$ . Further, there is a question of whether  $W/A$  and  $R$  should vary with  $L/D$ . In the

case of  $C_D$ , there is no question that  $C_D$  should decrease with increasing  $L/D$ , but only a question of how  $C_D$  should decrease. The particular variation chosen was that given by Newtonian hypersonic flow for a flat wing at high angles of attack. The stagnation-point radiative heating rates for lifting entry conditions are shown in figure 6. Maximum radiative heating rate per unit nose radius is plotted as a function of  $L/D$  for three selected values of weight-to-area ratio. The heating rate scale is logarithmic. The results are for  $L/D$  held constant during entry until zero flight-path angle is reached. Further, the entries are the single-pass undershoot type limited to a maximum deceleration of  $10g$ . With deceleration held constant with increasing  $L/D$ , a broadening of the entry corridor is obtained. For constant  $W/A$ , there is an order of magnitude increase in the radiative heating rate per unit nose radius in going from  $L/D = 0.5$  to  $L/D = 2.0$ . This increase is due to the fact that the higher  $L/D$  vehicle initially plunges deeper into the atmosphere, as a consequence of its lower drag coefficient and somewhat higher entry angle. Now a valid objection can be raised that the effect of  $L/D$  should not be compared at constant  $W/A$ . A reduction in  $W/A$  with increasing  $L/D$  undoubtedly would be more realistic. In fact, a low value of  $W/A$  appears to be essential if high stagnation point radiative rates are to be avoided at the higher values of  $L/D$ .

A  
5  
7  
3

These radiative rates for the lifting-entry case are compared in figure 7 with the corresponding convective rates. The ratio of the radiative heating rate to the convective rate per unit radius is plotted as a function of  $L/D$  for the previously selected values of  $W/A$ . A logarithmic ordinate scale is used. It is noted that the ratio increases by about an order of magnitude when  $L/D$  is increased from 0.5 to 2.0 at constant  $W/A$ . Again note the desirability of low  $W/A$  for the higher  $L/D$  values.

In addition to examining the stagnation point heating rates for lifting-entry vehicles, one should also examine heating rates at other points on the vehicles and the total heat absorbed by the heat shield. This is particularly necessary for high angle-of-attack entries. Unfortunately, such information is yet to be obtained.

Now consider these results from the standpoint of the design of heat-protection systems for parabolic-entry vehicles. It is apparent from the heating rate estimates that heat protection systems will be needed which are effective against both radiative and convective heating. A statement cannot be made, at this time, as to the complexity and weight penalty due to uncertainties in the radiative heating estimates and a lack of adequate information as to the reaction of heat-shield materials to combined radiative and convective heating. Of particular concern is the reaction of ablative materials which look very promising for protection against convective heating during parabolic entries. A point that needs to be mentioned about subliming ablative materials is that they are not likely to have as high an effective heat of ablation for

radiative heating as they have for convective heating. The high effective heat of ablation in the case of convective heating is largely due to the heat blocking effect of the vaporized materials. In the case of radiative heating, a heat blocking is not likely to occur unless the vaporized materials prove to be strongly absorbing.

#### CONCLUDING REMARKS

A  
5  
7  
3  
The assessment of the radiative heating problems can be summarized as follows. On the basis of available knowledge of the radiation from high-temperature air, it is concluded that radiative heat transfer will be important in the design of parabolic entry vehicles. The vehicle parameters influencing the radiative heating rates were determined and found to be the same as those for convective heating rates. These were nose radius, vehicle weight-to-area ratio, and drag coefficient. Their effect was greater in the case of radiative heating, and nose radius had an opposite effect. Conclusions cannot be drawn at present as to the influence of radiative heat transfer on vehicle shape, and heat-protection-system complexity and weight, because of uncertainties as to the radiant energy emitted from shock heated air, and a lack of information on the reaction of heat-shield materials to combined radiative and convective heating.

Ames Research Center

National Aeronautics and Space Administration

Moffett Field, Calif., April 11, 1960.

## APPENDIX A

## SUMMARY OF RADIATIVE HEATING ESTIMATES

## Basic Radiative Heating Rate Equation (Fig. 1)

In deriving the equation shown in figure 1, the following four assumptions were made: (1) the radiation intensity is uniform within the gas-cap volume radiating to the stagnation point, (2) radiation is not absorbed within the volume, (3) the stagnation point absorbs all of the incident radiation without any re-emission, and (4) the shock stand-off distance  $\delta$  is small compared to the nose radius  $R$ . The third assumption is equivalent to assuming that the stagnation point is a black body which is cold relative to the air in the gas cap. With these assumptions the radiative-heating rate can be expressed by the following equation:

A  
5  
7  
3

$$\dot{q}_r = \frac{E_t}{4\pi} \int_0^\tau \frac{\cos \theta}{r^2} d\tau$$

where  $r$  is the radius vector between an elemental gas volume and the stagnation point,  $\theta$  is the angle between the free-stream velocity and the radius vector, and  $\tau$  is the gas-cap volume radiating to the stagnation point. The equation reduces to the simple equation shown in figure 1 which is repeated here:

$$\dot{q}_r = \frac{\delta E_t}{2}$$

This equation applies to the radiation from a plane shock layer to a plane wall. With the fourth assumption (i.e.,  $\delta$  is small compared to  $R$ ), it is valid for the radiation from a spherical segment shock layer to the stagnation point of a spherical nose (i.e., the geometry shown in fig. 1). If the fourth assumption is not made, then the radiative heating rate for the geometry shown in figure 1 can be expressed as

$$\dot{q}_r = k_s \frac{\delta E_t}{2}$$

The factor  $k_s$ , termed the shape factor, thus is the ratio of the stagnation-point heating rate of a spherical nose to the heating rate per unit area of a plane wall.

## Procedures and Data Used in Applying Basic Radiative Heating Rate Equation

In applying the equation to a particular entry trajectory it is necessary to determine the relation between velocity and altitude and the associated values of atmospheric and gas-cap densities and temperatures. With this information, values of  $\delta$  and  $E_t$  can then be determined. The trajectory calculations were made by the use of Chapman's approximate analytical method of studying entry motion (ref. 1). In determining the densities and temperatures of the shock-heated air, the assumption was made that the heated air was in equilibrium. The equilibrium values of densities and temperatures at the required velocity and altitude conditions were obtained from reference 2. Shock standoff distances were evaluated by the following expression which was derived by Hayes (ref. 3):

$$\frac{\delta}{R} = \frac{\rho_1/\rho_2}{1 + \sqrt{2\rho_1/\rho_2}}$$

where  $\rho_1$  is the atmospheric density and  $\rho_2$  is the equilibrium shock-layer density. The values of  $E_t$  for equilibrium conditions were obtained from charts of  $E_t/2$  which were presented in reference 4.

### Accuracy and Limitations of the Radiative Heating Estimates

In determining the accuracy and limitations of the estimates there are four principal questions that need to be answered. These are: (1) For what conditions is it valid to assume that equilibrium conditions exist in the gas cap? (2) For what conditions is it valid to assume that the radiation intensity is uniform and that no absorption of radiation occurs within the gas cap? (3) What is the probable accuracy of the values of  $E_t$  used? (4) What is the probable accuracy of the estimates of the shock standoff distances?

Figure 8 is useful in considering these questions. The figure is a velocity-altitude map on which important regions have been indicated. In the upper right of the figure, portions of the velocity-altitude variations for two representative parabolic velocity entries are shown. The region of stagnation-point maximum radiative heating rates for single-pass, 10-g undershoot entries at parabolic velocity is also indicated; for these entries, the maximum radiative heating rate occurred at approximately 34,000 feet per second. The altitude-velocity boundary labeled "Radiative relaxation distance = Shock standoff distance,  $R = 1$  foot" is useful in considering the validity of the assumption that the shock-heated air is in equilibrium. This boundary was based on an extrapolation of radiative

relaxation rate data obtained from shock-tube measurements (ref. 5) at conditions corresponding to lower velocities and altitudes than those for parabolic velocity entries. In view of the extrapolation required, the boundary is very approximate at velocities near parabolic entry. For a nose radius other than 1 foot, a boundary can be determined roughly by the relation  $\rho_1 R = \text{Constant}$ . The boundary is useful in the following way. If the maximum radiative rate predicted on the assumption of equilibrium conditions occurs at an altitude that is either at or above the boundary, then the equilibrium assumption is invalid, since non equilibrium conditions exist throughout the shock layer except near the wall. At some lower altitude, equilibrium will be reached at a short enough distance behind the shock front for nonequilibrium radiation effects to be unimportant. At the present time, not enough is known about nonequilibrium radiation to permit this lower boundary to be defined. The second question, regarding the validity of the assumption of uniform radiation intensity and no absorption within the gas cap, is answered by comparing the altitude below which radiation decay and absorption become important. A larger radius is the more critical in this case; hence the boundary is shown for the largest nose radius considered, a 10-foot radius. If the altitude for the maximum radiative heating rate, based on the assumption of uniform radiation and no absorption, lies above this boundary, then the assumption is valid. This boundary where radiation decay and absorption become important is based on the results of an unpublished analysis by Dean R. Chapman and Kenneth K. Yoshikawa of the Ames Research Center. Examining the question as to the probable accuracy of the equilibrium values of  $E_t$  used, it can be seen from figure 8 that the region of maximum radiative heating rates for the parabolic entries considered is well outside the region covered by AVCO shock-tube measurements. Thus, as mentioned in the main part of the paper, values of  $E_t$  determined by theoretical extrapolations were used. (It should be mentioned that, even for the region denoted as AVCO air radiation data, the values of  $E_t$  were based on theory as modified by a limited number of measurements spread over the designated region.) There is considerable uncertainty as to the accuracy of these extrapolated values of  $E_t$ ; the present best guess is a factor of uncertainty of two. In the case of the values of shock standoff distances, no experimental check of the values given by Hayes' relation has been obtained at conditions approaching those for parabolic entry velocities. Comparison of predicted and measured values at lower velocities, however, has indicated agreement within 10 percent.

A  
5  
7  
3

#### Radiative Heating Rate Values for a Range of Velocities and Altitudes

Presented in figure 9 are values of stagnation-point radiative heating rates for a wide range of velocities and altitudes. The values were estimated by use of the procedures and data previously described and are subject to the limitations and uncertainties just described. In figure 10,

these radiative heating rates are compared with the corresponding equilibrium laminar convective heating rates. The convective heating rates were calculated by the method given in reference 1.

Maximum Radiative and Convective Heating Rates for  
Specific Parabolic Velocity Entries

The empirical equations for maximum radiative and convective heating rates which were given in figures 2 and 3, respectively, have certain restrictions as to their application. They apply only to single-pass, nonlifting, parabolic-velocity entries which are limited to a maximum deceleration of 10 g.

A  
5  
7  
3

## APPENDIX B

## SYMBOLS

## Heating Rate Estimates

A	vehicle reference area, sq ft	
$C_D$	vehicle drag coefficient based on A	A
$E_t$	total energy radiated per unit time per unit volume in gas cap, Btu/sec-cu ft	5
$k_s$	shape factor (see appendix A)	7
$\dot{q}$	stagnation-point heating rate, Btu/sec-sq ft	3
R	vehicle nose radius, ft	
r	radius vector from unit volume in gas cap to stagnation point, ft	
$\bar{V}$	ratio of entry velocity to satellite velocity	
W	vehicle weight, lb	
$\delta$	shock standoff distance, ft	
$\theta$	angle between radius vector r and flight velocity vector, deg	
$\rho$	mass density of air, slugs/cu ft	
$\tau$	volume of gas cap radiating to stagnation point, cu ft	

## Subscripts

r radiative

c convective

1 ahead of shock wave

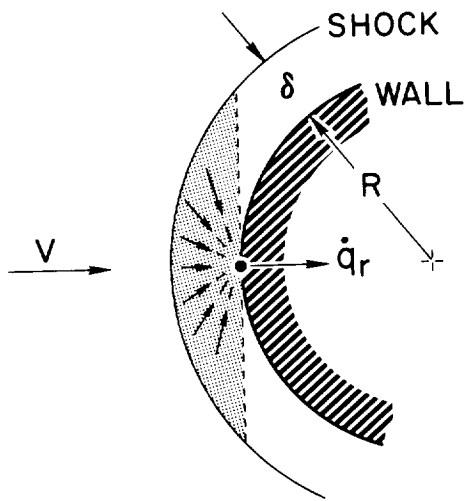
2 behind shock wave

A  
5  
7  
3

## REFERENCES

1. Chapman, Dean R.: An Analysis of the Corridor and Guidance Requirements for Supercircular Entry Into Planetary Atmospheres. NASA TR R-55, 1960.
2. Hochstim Adolf R.: Gas Properties Behind Shocks at Hypersonic Velocities. I. Normal Shocks in Air. Rep. No. ZPh(GP)-002, CONVAIR, Jan. 30, 1957.
3. Hayes, Wallace D.: Some Aspects of Hypersonic Flow. The Ramo-Wooldridge Corp., Jan. 4, 1955.
4. Kivel, B., and Bailey, K.: Tables of Radiation From High Temperature Air. Res. Rep. 21 (Contracts AF 04(645)-18 and AF 49(638)-61), AVCO Res. Lab., Dec. 1957.
5. Camac M., Camm, J., Keck, J., and Petty, C.: Relaxation Phenomena in Air Between 3000 and 8000° K. Res. Rep. 22 (Contract AF 04(645)-18), AVCO Res. Lab., Mar. 1958.

A  
5  
7  
3



RADIATIVE HEATING RATE:

$$\dot{q}_r = \left( \frac{\delta E_{\dagger}}{2} \right)$$

WHERE:

$\delta$  = SHOCK STANDOFF, FT  
 $E_{\dagger}$  = TOTAL RADIATION ENERGY RATE PER UNIT VOL, Btu/SEC-FT<sup>3</sup>

Figure 1.- Geometry and equation for radiative heating.

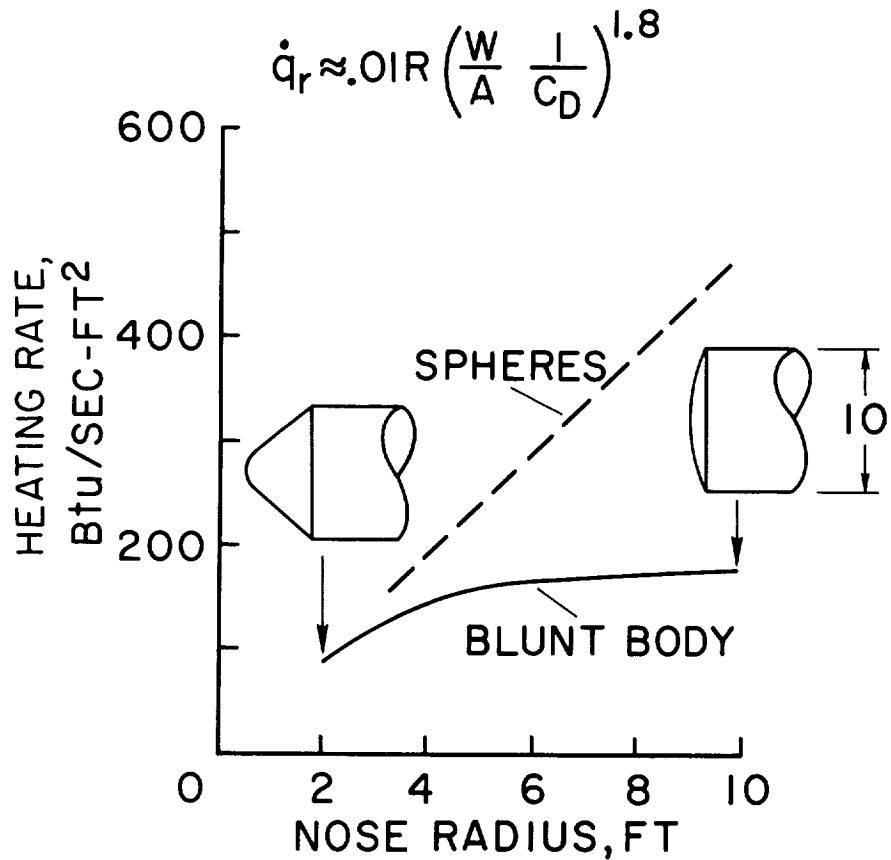


Figure 2.- Stagnation point maximum radiative heating rates;  $L/D = 0$ ,  $\bar{V} = \sqrt{2}$ ,  $W/A = 100$ .

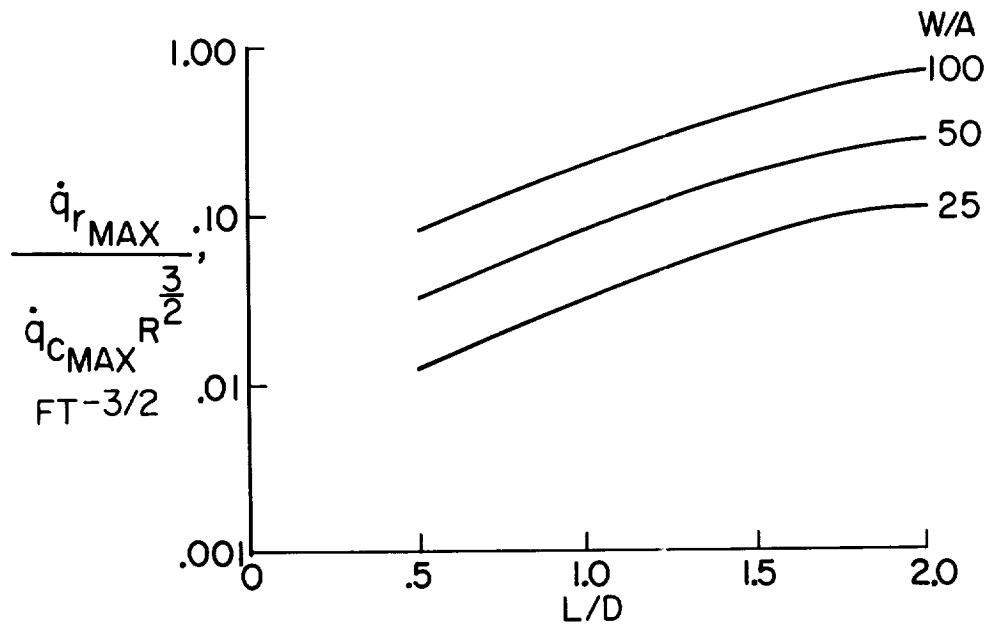


Figure 7.- Ratio of maximum radiative-to-convective heating rates for lifting entry;  $\bar{V} = \sqrt{2}$ .

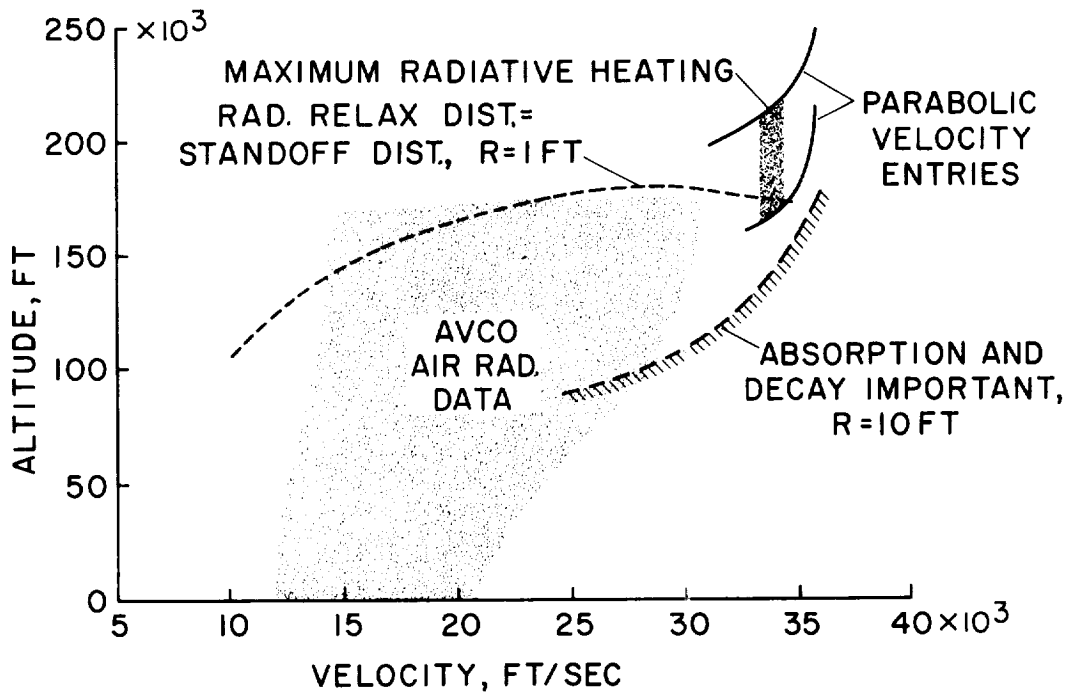


Figure 8.- Important velocity-altitude regions.

A  
5  
7  
3

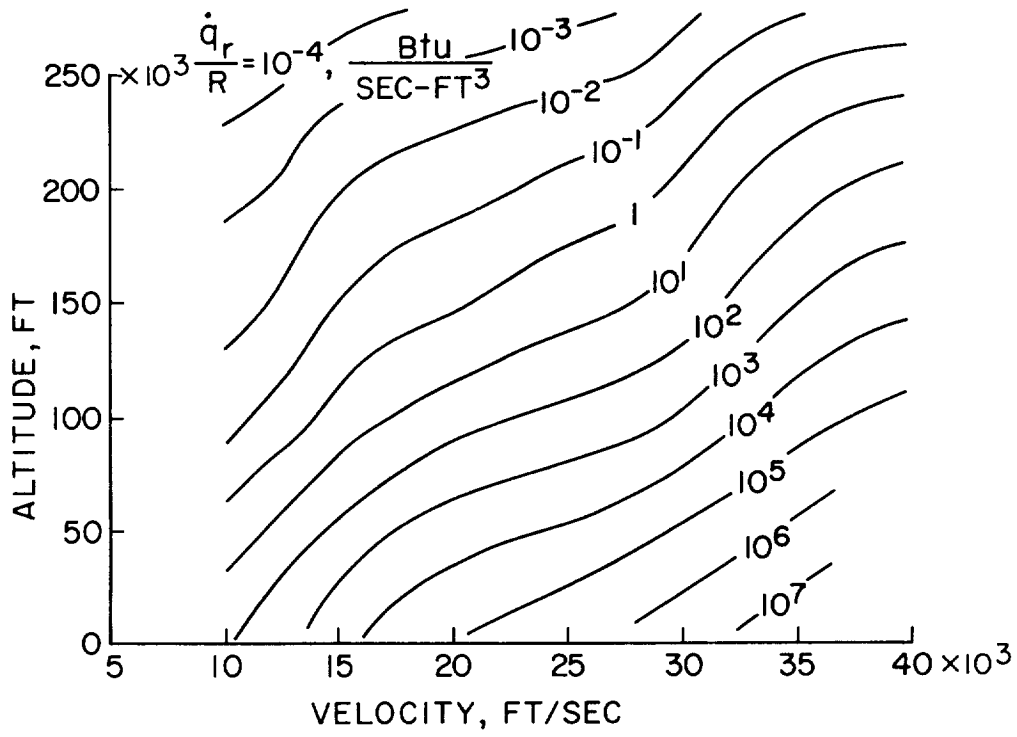


Figure 9.- Radiative heating.

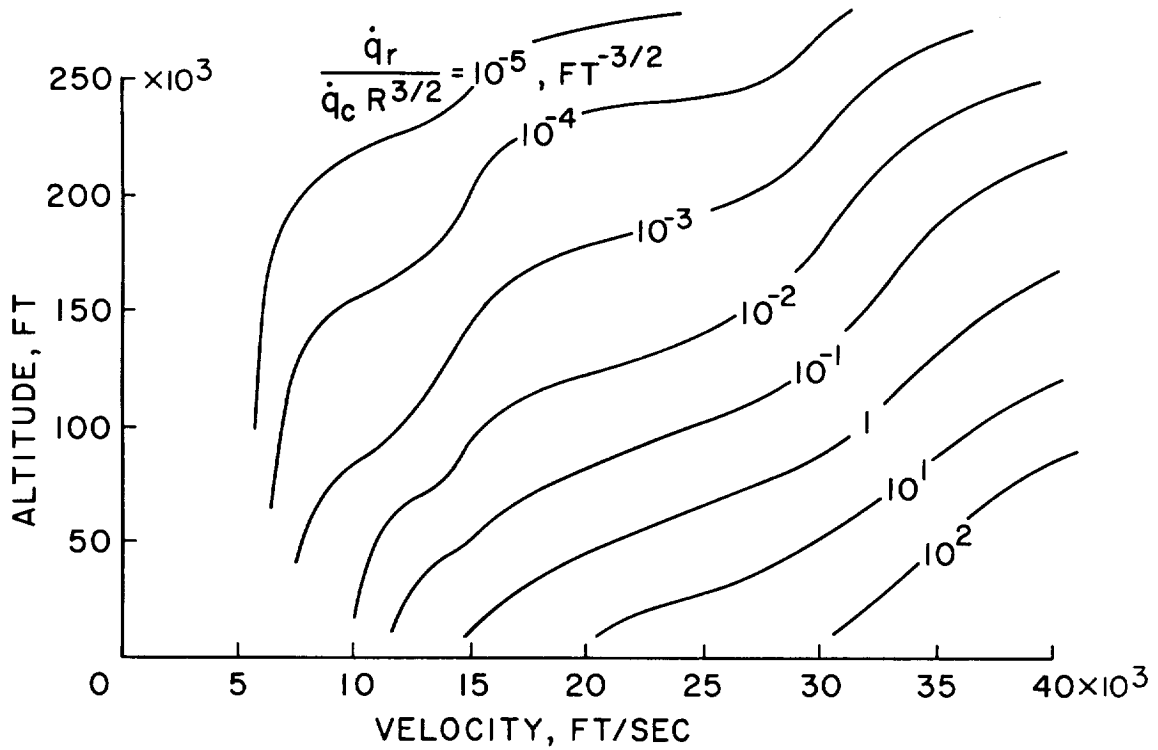


Figure 10.- Ratio of radiative to convective heating.

